

## Origin of dissipative losses in negative index of refraction materials

R. B. Gregor,<sup>a)</sup> C. G. Parazzoli, K. Li, and M. H. Tanielian  
Boeing Phantom Works, Seattle, Washington 98124

(Received 6 November 2002; accepted 28 January 2003)

Negative index of refraction materials have been postulated for many years but have only recently been realized in practice. In the microwave region these materials are constructed of rings and wires deposited on a dielectric substrate to form a unit cell. We have constructed, experimentally characterized, and simulated several of these structures operating in the 10–16 GHz range. The origin of the dissipative losses has been identified and effective schemes to reduce them devised and implemented. Numerical simulation and experimental verification shows that losses in negative index of refraction materials can be significantly reduced by minimizing the underlying losses of the constituent materials. © 2003 American Institute of Physics. [DOI: 10.1063/1.1563726]

Veselago<sup>1</sup> postulated the existence of a negative index of refraction material (NIM) in 1968. In the last few years NIMs have been realized by the combination of ring and wire conductive elements deposited on a dielectric substrate.<sup>2,3</sup> NIMs have the property that the effective permittivity, permeability, and refractive index are negative.<sup>1</sup> Consequences of these properties are that positive lenses become negative, flat sheets of NIMs focus and super lenses<sup>4</sup> might be formed with resolution at subwavelength scales. For such applications it is necessary to have NIMs with good transmission. In the original<sup>2</sup> structures used for NIMs, concerns<sup>5</sup> were raised due to the introduction of metals into the structure possibly creating unavoidable losses that would circumvent any characterization of a net negative real refractive index. In this letter we show that these concerns are not as significant as first suggested and we describe not only the origin of the losses in NIMs but also methods to reduce them.

A NIM contains a large number of unit cells similar to the one shown in Fig. 1 for the 901 HWD structure. The 901 HWD structure was part of this study in which several different geometries were simulated, experimentally measured and designated as 901, 402, etc. An efficient numerical modeling approach for these structures is to solve Maxwell's equations in a unit cell with appropriate boundary conditions. The types of boundary conditions available are open, electrical (EBC), magnetic (MBC), and periodic (PBC). The choice of the boundary conditions is a function of the procedure used to assemble the cells to generate the bulk NIM. If the cells are assembled so that symmetric conditions in the direction of the electric and magnetic fields are preserved, then EBC and MBC boundary conditions along  $z$  and  $y$ , respectively, are needed. If the symmetry is violated, then PBC conditions are required. In the course of this work both symmetric and asymmetric structures were modeled. A commercial code, Microwave Studio,<sup>3</sup> was used to perform the modeling and scattering parameter calculations for  $S_{11}$  (reflection) and  $S_{21}$  (transmission) in the elementary cell. The scattering parameters of a single cell can be cascaded to obtain the parameters of multiple cells. Numerical simulations

of one and three cells have shown that this approach is sufficiently accurate.

The experimental characterization of our NIM samples was performed in a free-space focused beam setup using an HP8510C network analyzer. Typically, the samples have a copper ring pattern deposited on one face of a dielectric substrate and a wire pattern on its opposite face. A wire is patterned on a separate substrate and interposed between two substrates having the ring/wire combination. A low loss dielectric spacer follows each of the substrates bearing the copper patterns.

The losses relate to the conductivity of the metallic layer, the dielectric materials used for substrate/spacers and the ad-

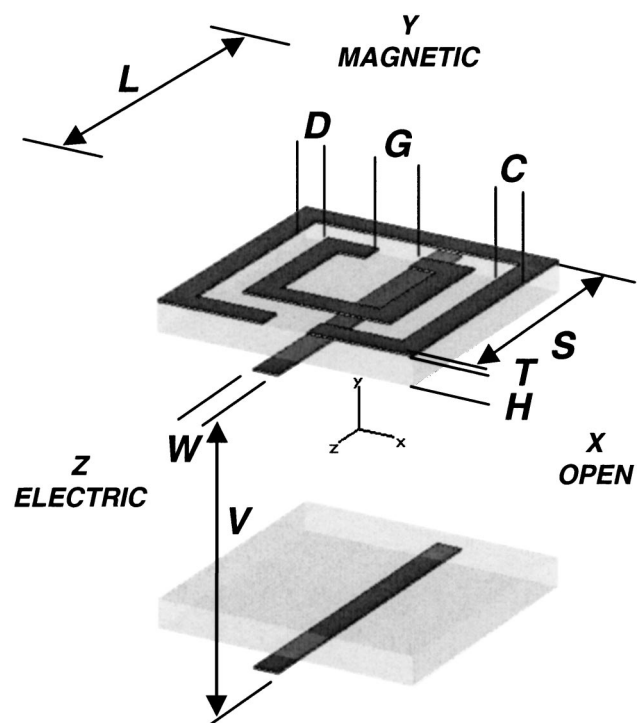


FIG. 1. Unit cell showing EBC, MBC, and the dimensions of the 901 HWD structure examined in this study. The direction of propagation of the electromagnetic field is along the  $x$  axis, the electric field along the  $z$  axis, and the magnetic field along the  $y$  axis. For the 901 HWD structure  $C = 0.025$  cm,  $D = 0.030$  cm,  $G = 0.046$  cm,  $H = 0.0254$  cm,  $L = 0.33$  cm,  $S = 0.263$  cm,  $T = 17.0 \times 10^{-4}$  cm,  $W = 0.025$  cm, and  $V = 0.255$  cm.

<sup>a)</sup>Electronic mail: robert.b.gregor@boeing.com

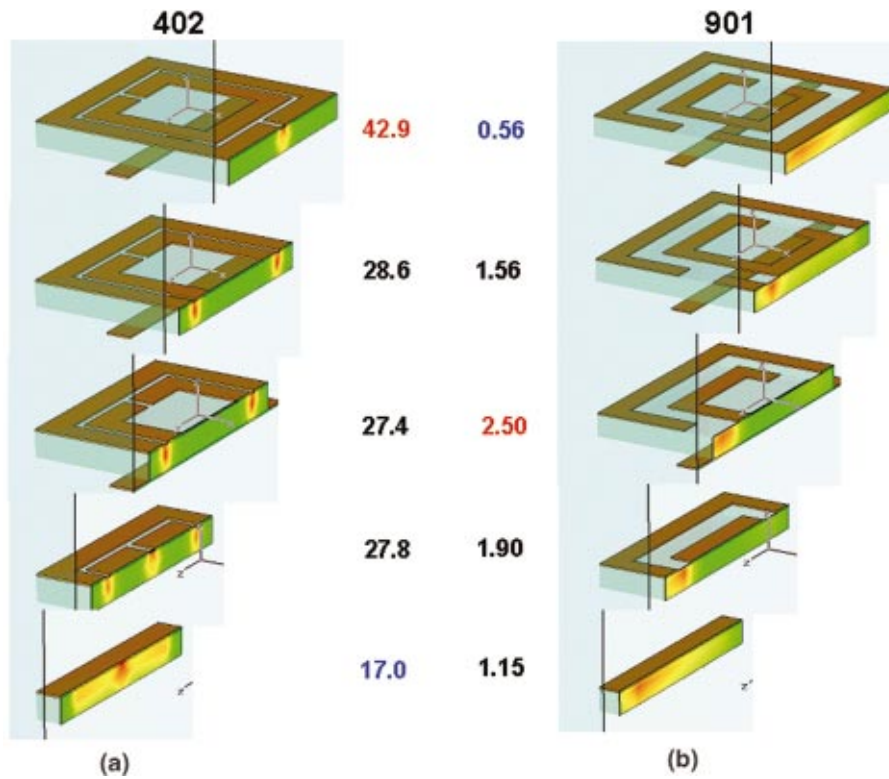


FIG. 2. (Color) Simulated (using EBC, MBC) power loss density for (a) the 402 structure and (b) the 901 structure. The 901 structure does not have the additional wire at the bottom of the 901 HWD unit cell as shown in Fig. 1. The numbers in the diagram indicate the maximum power loss density (a.u.) at each cut plane. For the 402 structure,  $C=0.025$  cm,  $D=0.0075$  cm,  $G=0.010$  cm,  $H=0.0254$  cm,  $L=0.33$  cm,  $S=0.215$  cm, and  $T=17 \times 10^{-4}$  cm.

hesives used to hold the structure together. Also, we have noted in our simulations that symmetric structures, where EBC and MBC are used, tend to exhibit higher transmission than asymmetric structures. This observation has not been experimentally tested, however. The dielectric losses are concentrated in the high field regions, as the power loss density numerical simulations clearly show in Fig. 2, for the 402 and 901 structures. The 901 structure differs from the 901 HWD shown in Fig. 1 by the absence of the lower wire and spacer. The power loss, in MKS units, is defined as  $P_L = P_D + P_w$ , where

$$P_D = \pi f (\tan \delta) \epsilon_0 \epsilon \int |E|^2 dV$$

is the dielectric loss and

$$P_w = \frac{1}{2} \sqrt{\frac{\pi \mu f}{\sigma}} \int |H|^2 dS$$

is the surface loss. Here  $\tan(\delta)$  is the loss tangent, defined as  $\tan \delta = \epsilon''/\epsilon'$ , where  $\epsilon = \epsilon' - i\epsilon''$ ,  $\mu$  is the permeability,  $f$  is the frequency, and  $\sigma$  is the metal conductivity. The values in Fig. 2 are not absolute and are only for relative comparison purposes. These results show that the small gaps concentrate the fields increasing the losses. The losses are limited to narrow regions surrounding the gaps. The 402 structure, which has an azimuthal gap 4.6 times smaller than the 901 structure, has a maximum power loss density  $\sim 17$  times higher. The removal of lossy dielectrics in the region of high fields significantly reduces the losses.

We define the insertion loss for the sample as  $l = 1 - (S_{11}S_{11}^* + S_{21}S_{21}^*)$ . For the results presented here the inser-

tion loss was calculated at the peak of the passband where  $S_{11}$  is very small and the NIM is well matched to free space so that multiple internal reflections are not significant. The simulated insertion loss,  $l$ , as function of the dielectric loss tangent ( $\tan \delta$ ), is shown Fig. 3 for the 901 and 402 structures. Comparing Fig. 3(a) and 3(b) we see that smaller ring gaps, resulting in higher electric fields, lead to higher losses. Also, the loss decreases with  $\tan \delta$ . The loss is highest when the dielectric completely fills the cell (Cu full sub) but lower when the copper pattern resides on a substrate surrounded by air. The results for a perfect electrical conductor (PEC) on a substrate are given by the squares in Fig. 3. The copper conductive losses dominate at low values of the dielectric loss tangent. These trends have also been observed in our experiments. Our simulations show that the thickness of the metal-

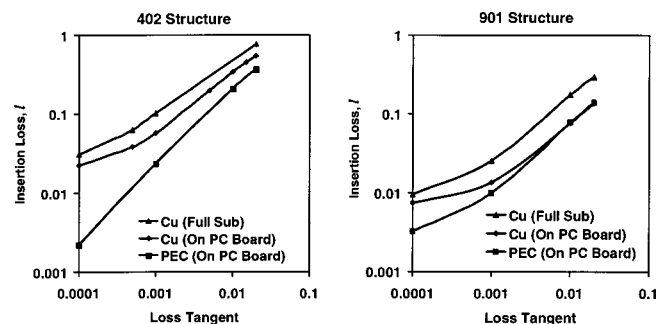


FIG. 3. Simulated (using EBC, MBC) losses at the passband peak for the (a) 402 and (b) 901 structures. Cu (full sub) stands for Cu embedded in a solid dielectric unit cell, whereas the Cu (on PC board) refers to a copper pattern on top of a substrate surrounded by air. PEC stands for a perfect electrical conductor.

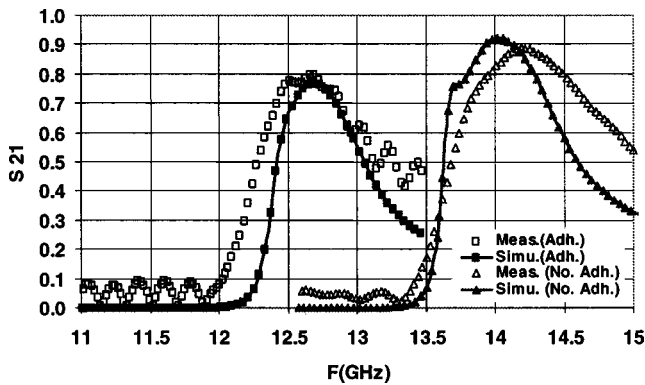


FIG. 4. Measured (open points) and simulated (solid points)  $S_{21}$  scattering parameters for 901 HWD structure with and without a 0.010 cm adhesive holding adjacent layers of NIM unit cells together. The simulations used PBC corresponding to the actual experimental samples. The adhesive had an  $\epsilon = 2.68$  and  $\tan \delta = 0.016$ .

lic layer also affects the insertion loss,  $l$ . Approximately 3–5 skin depths are needed to minimize the loss.

The method by which the layers are held together has a significant effect on the properties of the NIM. This effect can be observed by examining the results for two NIM structures with and without adhesive. For one 901 HWD sample we assembled the layers using an adhesive. An identical sample was assembled using tape on its surface, without using adhesive between the layers. The measured and simulated S-parameters are given in Fig. 4. The results show that when the adhesive is present, the peak of the passband is at  $\sim 12.7$  GHz with  $\sim 80\%$  transmission through three cells (1 cm). When the adhesive is absent and the structure is held together with tape at the sample perimeter, the peak of the passband moves to  $\sim 14.2$  GHz with  $\sim 90\%$  transmission through three cells. The effect of the adhesive is pronounced

due to its placement adjacent to the ring gaps where the electric field is high. Even though the thickness of the adhesive is only 0.010 cm, it shifts the passband by  $\sim 1.5$  GHz and decreases the transmission from  $\sim 90\%$  to  $\sim 80\%$ . Simulations show that if the adhesive is placed away from the gaps it has little effect on the NIM performance. These simulations and experimental results stress the importance of using low loss dielectric materials in the vicinity of the ring gaps.

In summary, we have investigated the losses in NIMs operating in the 10–16 GHz region. Low loss dielectric substrates are required especially in the vicinity of the ring gaps where the electric fields are high. We have used these guidelines to obtain transmission on the order of 90% for 1-cm-thick samples. This allows losses to approach the intrinsic dissipation in the metallic rings and wires. Insuring that metals are on the order of 3–5 skin depths thick minimizes the dissipation in the metallic components.

This work was supported by DARPA Contract No. MDA972-01-2-0016. We extend our thanks to V. Starkovich, S. Mclean, J. Nielsen, and A. Vetter from Boeing, S. Schultz and D. Smith from the University of California-San Diego, C. Soukoulis and P. Markos from Iowa State University, and R. Schuhmann and T. Weiland from Technical University of Darmstadt for useful discussions, suggestions, and help with various aspects of this work.

<sup>1</sup>V. G. Veselago, *Sov. Phys. Usp.* **10**, 509 (1968).

<sup>2</sup>D. R. Smith, W. Padilla, D. C. Vier, S. C. Nemat-Nasser, and S. Schultz, *Phys. Rev. Lett.* **84**, 4184 (2000).

<sup>3</sup>T. Weiland, R. Schuhmann, R. B. Greegor, C. G. Parazzoli, A. M. Vetter, D. R. Smith, D. C. Vier, and S. Schltz, *J. Appl. Phys.* **90**, 5419 (2001).

<sup>4</sup>J. B. Pendry, *Phys. Rev. Lett.* **85**, 3966 (2000).

<sup>5</sup>N. Garcia and M. Nieto-Vesperinas, *Opt. Lett.* **27**, 885 (2002).